Rapid Communication

Cation mixing $(Li_{0.5}Fe_{0.5})_2SO_4F$ cathode material for lithium-ion batteries*

Sun Yang(孙 洋), Liu Lei(刘 磊), Dong Jin-Ping(董金平), Zhang Bin(张 斌), and Huang Xue-Jie(黄学杰)†

Beijing National Laboratory for Condensed Matter Physics, Institute of Physics, Chinese Academy of Sciences, Beijing 100190, *China*

(Received 12 October 2011; revised manuscript received 21 October 2011)

We study the crystal structure of a triplite-structured $(Li_{0.5}Fe_{0.5})SO_4F$ with full Li^+/Fe^{2+} mixing. This promising polyanion cathode material for lithium-ion batteries operates at 3.9 V versus Li^+/Li with a theoretical capacity of 151 mAh/g. Its unique cation mixing structure does not block the Li^+ diffusion and results in a small lattice volume change during the charge/discharge process. The calculations show that it has a three-dimensional network for Li-ion migration with an activation energy ranging from 0.53 eV to 0.68 eV, which is comparable with that in $LiFePO_4$ with only one-dimensional channels. This work suggests that further exploring cathode materials with full cation mixing for Li-ion batteries will be valuable.

Keywords: lithium-ion battery, cathode material, triplite, cation mixing

PACS: 61.66.–f, 66.10.Ed, 71.15.Mb, 82.47.Aa **DOI:** 10.1088/1674-1056/20/12/126101

1. Introduction

Lithium-ion batteries are the enabling technology for electric vehicles and smart grids. The cathode material determines their energy and power densities.[1] $LiCoO_2$, $LiMn_2O_4$, $Li(Ni_xCo_{1-x})O_2$, $Li(Ni_xCo_yMn_{1-x-y})O_2$, $LiFePO_4$, etc., have been widely studied and applied in commercial batteries. For all those materials, a well-ordered cationic distribution is needed to ensure the fast lithium diffusion and thus the electrochemical activity. For layered structures, transition metal (T^M) ions occupying Li layers will cause a contraction of the inter-slab space, which is detrimental to the Li-ion transport through an increase in the activation energy.[2] In the case of olivine structured $LiFePO_4$, the well-known one-dimensional Li-ion channels are prone to be blocked by the T^M impurity presented in the Li sites.[3] The Cr^{3+} doped into $LiFePO_4$, which improves the electronic conductivity evidently, does not lead to an improved electrochemical performance because of this blocking effect.[4] Therefore, the conventional wisdom for good cathode material focuses on the synthesis of compounds with minimal defects.

Recently, we reported a monoclinic form of $LiFeSO_4F$ (m-$LiFeSO_4F$) with an insertion voltage of c.a. 3.9 V versus Li^+/Li,[5,6] higher than that (3.6 V) of its triclinic polymorph $LiFeSO_4F$ (t-$LiFeSO_4F$) proposed by Recham *et al.*[7] This material has a full Li/Fe site mixing, therefore it should be written as $(Li_{0.5}Fe_{0.5})_2SO_4F$. To the best of our knowledge, this is the first report of a compound with total site mixing which still exhibits an excellent electrochemical activity. Based on its crystal structure, we analysed its physical and chemical properties by using density functional theory (DFT) based *ab initio* calculation, which has been proved to be an effective method to study the materials for Li-ion batteries.[8–11] $(Li_{0.5}Mn_{0.5})_2SO_4F$, $(Li_{0.5}Co_{0.5})_2SO_4F$, and $(Li_{0.5}Ni_{0.5})_2SO_4F$ are also analyzed. The calculations are helpful to explore more cathode materials in this family.

2. Crystal structure

Using the Rietveld method implemented in the FullProf software suite,[12] the structure can be fully indexed to a monoclinic cell (space group $C2/c$), as shown in Fig. 1. The lattice constants are a = 13.0401(8) Å (1 Å=0.1 nm), b = 6.3914(4) Å, c = 9.8490(6) Å, β = 119.766(2), and V = 712.56(8) Å^3.

*Project supported by the National High Technology Research and Development Program of China (Grant No. 2009AA033101).
†Corresponding author. E-mail: xjhuang@iphy.ac.cn
© 2011 Chinese Physical Society and IOP Publishing Ltd

The atomic coordinates are listed in Table 1. The resultant crystal structure is isostructural to triplite Mn_2PO_4F[13] with a fully mixing of Li and Fe ions occupying two different crystallographic sites. As illustrated in Fig. 2, a unit cell of $LiFeSO_4F$ contains 8 formula units (f.u.). Two crystallographically independent Li/Fe sites are labeled as sites 1 and 2. The Li1/Fe1 and the Li2/Fe2 centered $(Li/Fe)O_4F_2$ octahedra are linked together by F–F or O–O edges alternately forming chains along [010] and [101] directions, respectively. These octahedral chains are bridged by isolated SO_4 tetrahedra creating a three-dimensional framework. Such a fully cation mixing of Li and T^M ions has never been seen before for the cathode material of the Li-ion battery. For the conventional cathode materials, e.g. olivine-structured $LiFePO_4$ or layered $LiNiO_2$ and $Li(Mn_xNi_{1-x})O_2$, even a small quantity of Li/T^M mixing (in other words, LiT^M anti-site defects) will lead to a poor electrochemical performance.[14–16] However, our electrochemical measurements show that m-$LiFeSO_4F$ is highly electrochemical active with an insertion voltage of c.a. 3.9 V versus Li^+/Li, and almost 100% of lithium can be extracted from the lattice. The reversibility and the cycleability are also acceptable.[5] To get further insight into this material, theoretically analyses are performed.

Table 1. Atomic coordinates for $(Li_{0.5}Fe_{0.5})_2SO_4F$ in the $C2/c$ space group. $R_{Bragg} = 16.05\%$, $R_f = 14.23\%$.

Atom	Wyckoff symbol	x/a	y/b	z/c	Occupancy
O1	8f	0.3646(7)	0.2808(13)	0.1369(9)	1.000
O2	8f	0.2109(8)	0.1401(15)	0.1909(8)	1.000
O3	8f	0.3068(6)	0.9157(15)	0.0857(9)	1.000
O4	8f	0.4214(8)	0.0265(12)	0.3608(10)	1.000
F1	8f	0.5129(6)	0.5938(12)	0.3892(7)	1.000
Li1	8f	0.5523(4)	0.7478(9)	–0.0039(6)	0.500
Li2	8f	0.3348(3)	0.3937(7)	0.6553(4)	0.500
Fe1	8f	0.5523(4)	0.7478(9)	–0.0039(6)	0.500
Fe2	8f	0.3348(3)	0.3937(7)	0.6553(4)	0.500
S1	8f	0.3281(4)	0.0947(8)	0.1973(5)	1.000

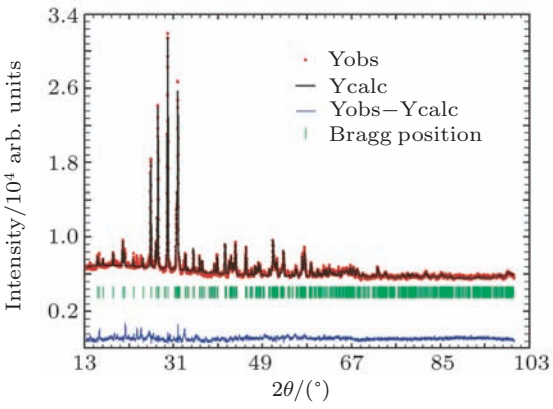


Fig. 1. (colour online) X-ray powder diffraction pattern (λ_{Cu}) of $(Li_{0.5}Fe_{0.5})_2SO_4F$, with the experimental data (red circles), calculated pattern (black line), Bragg positions (green markers), and difference curve (blue line). The X-ray diffraction (XRD) patterns were recorded by an X-ray diffract photometer (Rigaku Rint-2400) using CuK_α radiation ($\lambda_1 = 1.54053$ Å; $\lambda_2 = 1.54431$ Å) at a scan rate of 0.02° (2θ) s^{-1}. The refinement was done using the Fullprof program.

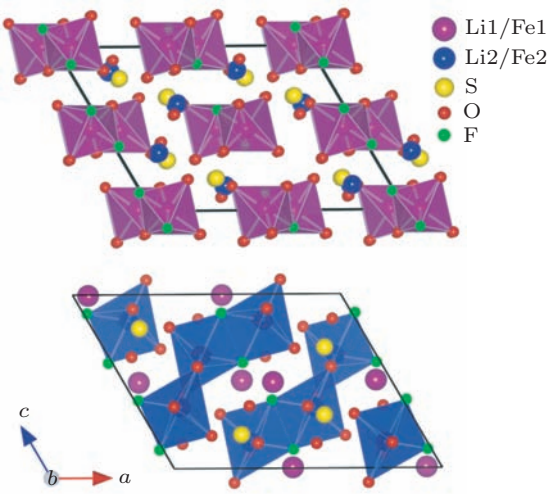


Fig. 2. (colour online) Refined structure of m-$LiFeSO_4F$. Purple, blue, yellow, red, and green balls represent Li1/Fe1, Li2/Fe2, P, O, and F atoms, respectively. Li1/Fe1 (upper one) and Li2/Fe2 (lower one) based $(Li/Fe)O_4F_2$ octahedra are drawn in purple and blue surfaces, respectively.

3. Computational details

The *ab initio* DFT calculations were done using the Vienna *ab initio* simulation package (VASP)[17,18] with the projector augmented wave method employed to describe the electron–ion interaction.[19] The Perdew–Wang 91 type generalized gradient approximation (GGA)[20] was used to describe the exchange–correlation potential. A Hubbard-type correction was taken into account due to the strongly correlated nature of the d electrons of the T^{M} atoms.[21,22] According to a previous literature,[8] effective U values of 4 eV, 4.5 eV, 5.5 eV, and 6 eV were adopted for Fe, Mn, Co, and Ni elements, respectively. For all the calculations, a large cut-off energy of 600 eV was used for the plane-wave expansion to ensure convergence. The integration over the reduced Brillouin zone was carried out with Γ-centered grids of 7×7×5 for t-LiT^{M}SO$_4$F and 3×5×4 for m–LiT^{M}SO$_4$F (T^{M} = Mn, Fe, Co, Ni). A full geometry optimization was performed for the structure relaxation. Both the activation energy and the migration pathway for lithium-ion diffusion in m-LiFeSO$_4$F were optimized using the nudged elastic band method (NEB).[23] The calculations of the average insertion voltages were according to the well-developed method.[24] As the magnetic ordering does not have any significant impact on the considering properties (comparable to tavorite-structured t-LiFeSO$_4$F),[25] the ferromagnetic magnetic sequence was adopted in all cases.

4. Results and discussion

For the unit cell of cation mixing m-LiFeSO$_4$F, many possible configurations with different Li/Fe orders exist. We choose the following model that can well reproduce the experimental insertion voltage: four Li ions occupy four of the eight Li1/Fe1 sites uniformly, and the other four Li ions occupy four of the eight Li2/Fe2 sites uniformly, then eight Fe ions occupy the remaining eight Li/Fe sites. Actually, this configuration is the most ideal lattice structure without any preferential segregation of Li or Fe atoms between the Li1/Fe1 and the Li2/Fe2 sites, which is closest to the fully mixing Li/Fe distribution. In this ideal configuration, as shown in Fig. 3, both LiO_4F_2 and FeO_4F_2 octahedra are linked together by fluorine vertices forming zig–zag chains along the [001] direction. The optimized lattice parameters agree well with the experimental values (Table 2). The computational results show that the lattice volume will shrink by 2% after the delithiation. In the XRD patterns shown in Fig. 4, four main characteristic peaks of m-LiFeSO$_4$F are nearly fixed at different stages of charge/discharge, indicating an even smaller volume change than the theoretical predicted value. In contrast, for a well-ordered structure, the computational results will underestimate the lattice volume change (calc. 7% versus exp. 10% for t-LiFeSO$_4$F[7] and calc. 4% versus exp. 7% for LiFePO$_4$.[26]) Considering the order model in our calculation, we attribute this underestimation of volume change of m-LiFeSO$_4$F to the disorder distribution of the Li ions in the real system. This small volume change is beneficial for keeping the electrode integrity during the charge/discharge process, which is vital for a long cycle life of Li-ion battery. The insertion voltage of m-LiFeSO$_4$F is calculated to be 3.91 V versus Li$^+$/Li, in accordance with our electrochemical measurements.[5] The formation energy of the Li–Fe antisite defect is calculated to be 0.15 eV, which is much lower than that of LiFePO$_4$ (more than 0.5 eV)[3,27,28] and t-LiFeSO$_4$F (2.50 eV).[29] Therefore, a fully Li/Fe mixing can be obtained when the material is synthesized at 380 °C.

Table 2. Comparison of experimental and calculated lattice parameters for $(Li_{0.5}Fe_{0.5})_2SO_4F$.

Parameter	Expt.	Calc.	Disparity
a/Å	13.0401	13.3314	2.2%
b/Å	6.3914	6.3843	0.1%
c/Å	9.8490	10.0446	2.0%
β/(°)	119.766	120.487	0.6%
Volume/Å^3	712.56	736.72	3.4%

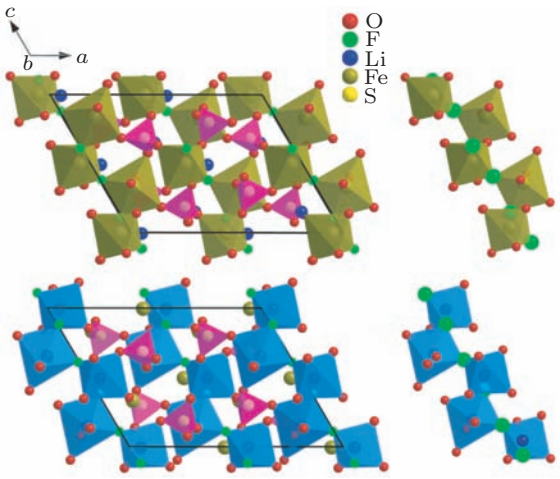


Fig. 3. (colour online) Structure model of m-LiFeSO$_4$F adopted during calculation. Li, Fe, S, O, and F atoms are represented with blue, dark yellow, yellow, red, and green balls, respectively. Fe–O–F octahedra (upper one) and Li–O–F octahedra (lower one) are plotted with dark yellow and blue color, respectively. Their corresponding one-dimensional chains are also plotted in the right column.

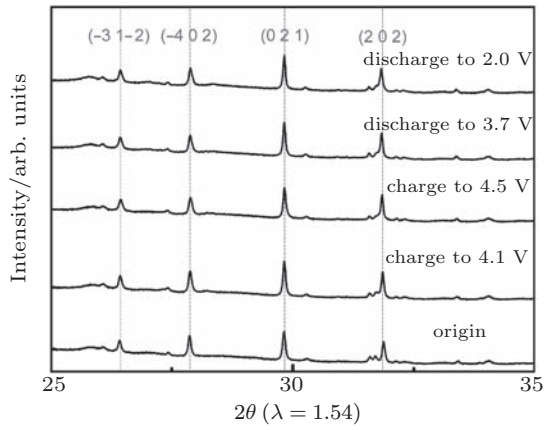


Fig. 4. Four main characteristic XRD peaks of $(Li_{0.5}Fe_{0.5})_2SO_4F$ at different charge/discharge stages. Minor evolution of diffraction peaks indicates slight volume change after (de)lithiation process.

For the Fe 3d electrons, the DFT+U calculation can well reproduce their electronic structure.[9] The calculated spin-polarized density of states (DOS) and the projected density of states (PDOS) for m-$LiFeSO_4F$ and m-$FeSO_4F$ are shown in Fig. 5. Both of them appear to be insulators with band gap values of 3.4 eV and 1.9 eV for m-$LiFeSO_4F$ and m-$FeSO_4F$, respectively. It is shown that the valence band maximum (VBM) of m-$LiFeSO_4F$ and the conduction band minimum (CBM) of m-$FeSO_4F$ are mainly projected on the Fe ions, indicating the charge transfer is mainly localized around the Fe ions during the charge/discharge process, which is similar to $LiFePO_4$.[9] The Barder charge analysis[30–32] shows a 0.51 electron loss of the Fe ion after the delithiation, which is also comparable to that of $LiFePO_4$. Therefore, a small polaron mechanism analogous to that of $LiFePO_4$[33] is expected for the electrons transportation in m-$LiFeSO_4F$.

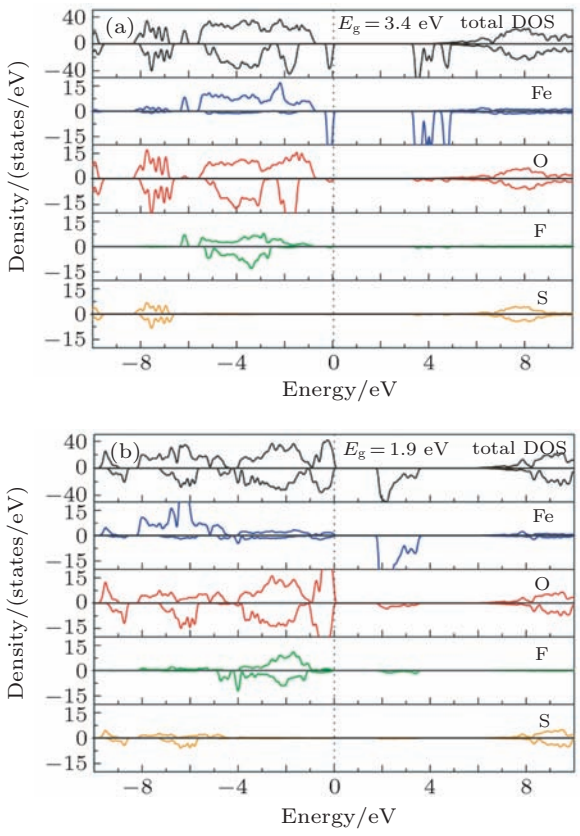


Fig. 5. (colour online) DOS (density of states) and PDOS (projected density of states) of m-$LiFeSO_4F$ (a) and m-$FeSO_4F$ (b). Fermi level is put at 0 eV.

The lithium-ion diffusion is normally the rate determining step for the electrochemical process in charge/discharge of a Li-ion battery. For the tavorite-structured t-$LiFeSO_4F$, the lithium transportation mechanism is disputable. Liu and Huang's calculation indicated a one-dimensional (1D) lithium-ion channel,[34] while Tripathi *et al.* predicted it to be a three-dimensional (3D) conductor.[29] Recently, Muller *et al.* reported a 1D lithium migration pathway in the tavorite-structured material.[35] Here we investigate possible diffusion paths for lithium migration in m-$LiFeSO_4F$, and the activation energies are calculated accordingly. Five possible lithium migration paths (three inner-chain paths and two inter-chains paths, figures 6(a)–6(e)) are considered, and the computational results indicate a quasi-3D network for lithium-ion transportation exist with an activation energy ranging from 0.53 eV to 0.68 eV (Fig. 7). Considering the unique Li/Fe mixing occupation in this compound, we also simulate the process of one Fe ion migrating into a nearest Li-vacancy site, and the result indicates that the Fe ion is relatively stable because the activation energy for Fe^{2+} diffusion is 0.9 eV (Fig. 6(f)). It can be assumed that Fe^{3+} formed after Li extraction undertakes an even larger electrostatic repulsive force on the migration path and therefore has a much lower diffusion coefficient. Hence we may infer that the Fe ion is stable in the electrochemical process. It should be stressed that we adopt an ideal configuration in these calculations. We can reasonably expect that other configurations deviating from this model, where the Fe ions may hinder the Li^+ migration, will at worst impede the lithium diffusion in a localized region but Li^+ can always find its way in the 3D channels. This explains why this fully cation mixing electrode material still shows a satisfying electrochemical performance. Nevertheless, further investigations, experimentally and theoretically, are still needed to further clarify the lithium diffusion mechanism in this full cation mixing system.

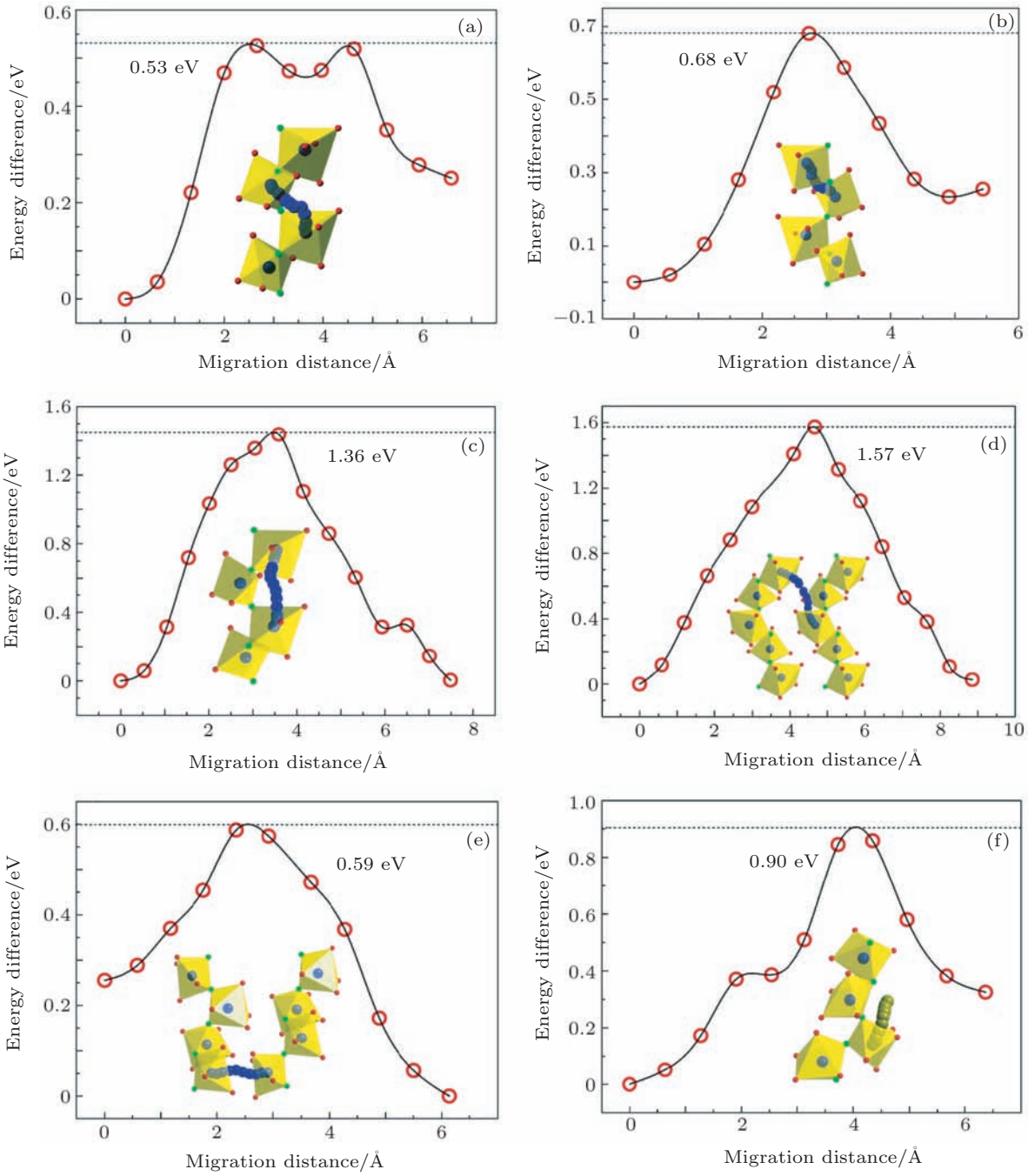


Fig. 6. (colour online) (a)–(e) Optimized channels and activation energies for lithium-ion migration. Related Li–O–F octahedral chains are plotted in the picture, (f) Fe atom migrates onto the nearest Li vacancy.

Besides t-$LiFeSO_4F$, Barpanda *et al.* have also reported the synthesis of $LiT^{M}SO_4F$ (T^{M} = Mn, Co, Ni) compounds.[36] Among them $LiCoSO_4F$ and $LiNiSO_4F$ share the same structure with t-$LiFeSO_4F$, while $LiMnSO_4F$ is isostructural to m-$LiFeSO_4F$. For comparison, we perform calculations on $LiT^{M}SO_4F$ (T^{M} = Mn, Fe, Co, Ni) of both triclinic and monoclinic phases. In all cases, as shown in Table 3, t-$LiT^{M}SO_4F$ seems to be more energetically favorable. Whereas it should be noted that the approximation, $G = E + PV - TS \approx E$, is valid only when both PV and TS are negligible, where G, E, T, S, P, and V represent the Gibbs free energy, the internal energy, the temperature, the entropy, the pressure, and the volume, respectively. Under ambient pressure, PV is negligibly small, while TS should be considered since the ionic disorder will contribute a configurational entropy. In t-$LiFeSO_4F$, every Li ion occupies two close sites with equal probability, which will lead to an entropy of $\ln 2 * k_B$ per f.u., where k_B is the

Boltzmann constant. In the case of m-$LiFeSO_4F$, a thorough mixing occupations of Li and Fe ions will result in an entropy of $2\ln 2 * k_B$ per f.u. For simplicity, other degrees of freedom, e.g., electronic entropy, which might cause a small quantitative correction, are neglected. After taking into account the configurational entropy, the triclinic phase is more energetically favorable for $LiFeSO_4F$, $LiCoSO_4F$, and $LiNiSO_4F$, while the monoclinic phase is more stable for $LiMnSO_4F$. This explains why m-$LiMnSO_4F$ not t-$LiMnSO_4F$ is obtained through the same synthesis method. In addition, our calculation indicates that m-$LiFeSO_4F$ is in a metastable state compared to t-$LiFeSO_4F$. It is indeed reflected in our synthesis. In contrast with the readily available pure phase m-$LiMnSO_4F$, as-prepared m-$LiFeSO_4F$ is very sensitive to the preparation conditions (temperature, pressure, etc.). The computational results indicate that both m-$LiCoSO_4F$ and m-$LiNiSO_4F$ might also be synthesized.

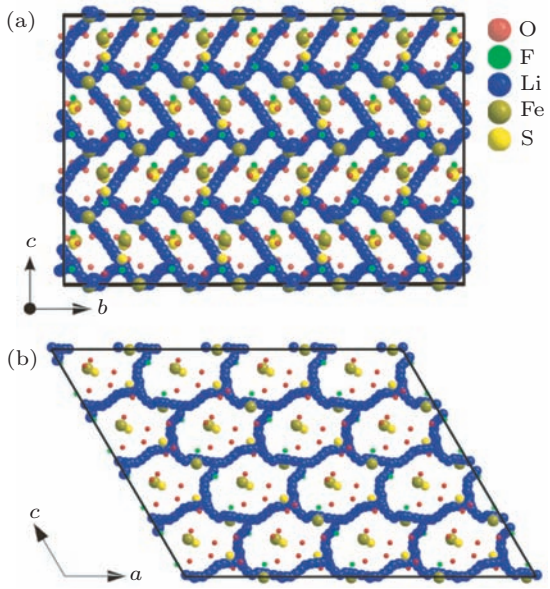


Fig. 7. (colour online) Three-dimensional transportation network for lithium-ion transportation from the perspective of a and b axes. Only the migration paths with activation energy less than 0.7 eV were plotted.

Table 3. Calculated internal energies and Gibbs free energies of t-$LiMSO_4F$ and m-LiT^MSO_4F (T^M = Mn, Fe, Co, Ni) per formula unit. $\Delta E(G)$ is defined as $E(G)[m\text{-}LiT^MSO_4F]$–$E(G)[t\text{-}LiT^MSO_4F]$. Positive (negative) value indicates t-$LiMSO_4F$ (m-$LiMSO_4F$) is more energetically favorable. In the calculation of Gibbs free energy, a temperature of 600 K, which is close to the synthesis condition, is adopted.

	E^t/eV	E^m/eV	ΔE/meV	G^t/eV	G^m/eV	ΔG/meV
$LiMnSO_4F$	–50.055	–50.038	+17	–50.091	–50.110	–19
$LiFeSO_4F$	–48.106	–48.049	+57	–48.142	–48.121	+21
$LiCoSO_4F$	–45.974	–45.916	+58	–46.010	–45.988	+22
$LiNiSO_4F$	–44.367	–44.262	+105	–44.403	–44.334	+69

The calculated insertion voltage of m-$LiMnSO_4F$ is 4.75 V versus Li^+/Li, but no capacity was detected in our electrochemical tests. This may be due to its extremely poor kinetic properties caused by the well-known sluggish Mn^{2+}/Mn^{3+} redox couple, which has been observed in $LiMnPO_4$.[37,38] Making nano-size powders and surface coating with conducting layers may improve its electrochemical activity. The calculated insertion voltage of m-LiT^MSO_4F is always higher than those of t-LiT^MSO_4F and LiT^MPO_4, as summarized in Table 4. As far as we know, 3d transition mental redox couples exihibit the highest electric potential under this triplite like structure. Based on the existing technologies, applications of both m-$LiCoSO_4F$ and m-$LiNiSO_4F$ should be difficult due to the high voltage plateau, which is far beyond the electrochemical window of any conventional electrolytes.

Table 4. Calculated insertion voltages (versus Li^+/Li) for LiT^MPO_4, t-LiT^MSO_4F, and m-LiT^MSO_4F (T^M = Mn, Fe, Co, Ni). Available experimental voltage are given in parentheses.

	LiT^MPO_4[a]	t-LiT^MSO_4F	m-LiT^MSO_4F
Mn	4.1 V (4.1 V)	4.4 V	4.7 V
Fe	3.5 V (3.45 V)	3.7 V (3.6V[b])	3.9 V (3.9 V[c])
Co	4.7 V (4.8 V)	4.9 V	5.2 V
Ni	5.1 V	5.4 V	5.6 V

[a]Ref. [8], [b]Ref. [7], [c]Ref. [5].

5. Conclusion

In summary, we reported the crystal structure of monoclinic phase $(Li_{0.5}Fe_{0.5})_2SO_4F$ and investigated this framework by using the first principles calculations. It has the properties of a high insertion voltage, a quasi-3D Li-ion transportation network, and a small lattice volume change during the charge/discharge process, which make it a promising cathode material

for the rechargeable lithium-ion battery. Its unique cation mixing property provides a new perspective in the hunt for better positive electrode materials. We expect upcoming researches on this new framework will lead to better cathode materials for lithium-ion batteries.

References

[1] Tarascon J M and Armand M 2001 *Nature* **414** 359

[2] Kang K, Meng Y S, Bréger J, Grey C P and Ceder G 2006 *Science* **311** 977

[3] Malik R, Burch D, Bazant M and Ceder G 2010 *Nano Lett.* **10** 4123

[4] Li H, Wang Z X, Chen L Q and Huang X J 2009 *Adv. Mater.* **21** 4593

[5] Liu L, Zhang B, Li H and Huang X J 2011 *Prog. Nat. Sci.* **21** 211

[6] Liu L, Zhang B, Li H and Huang X J 2011 *18th International Conference on Solid State Ionics*, Warsaw, Poland, July 3–8, 2011 p. 375

[7] Recham N, Chotard J N, Dupont L, Delacourt C, Walker W, Armand M and Tarascon J M 2010 *Nat. Mater.* **9** 68

[8] Zhou F, Cococcioni M, Marianetti C A, Morgan D and Ceder G 2004 *Phys. Rev.* B **70** 235121

[9] Zhou F, Kang K, Maxisch T, Ceder G and Morgan D 2004 *Solid State Commun.* **132** 181

[10] Zhou F, Cococcioni M, Kang K and Ceder G 2004 *Electrochem. Commun.* **6** 1144

[11] Zhou F, Maxisch T and Ceder G 2006 *Phys. Rev. Lett.* **97** 155704

[12] Rodríguez-Carvajal J 1993 *Physica* B **192** 55

[13] Rea J R and Kostiner E 1972 *Acta Cryst.* B **28** 2525

[14] Yang S, Song Y, Ngala K, Zavalij P Y and Whittingham M S 2003 *J. Power Sources* **119** 239

[15] Rougier A, Gravereau P and Delmas C 1996 *J. Electrochem. Soc.* **143** 1168

[16] Rossen E, Jones C and Dahn J 1992 *Solid State Ionics* **181** 1209

[17] Kresse G and Furthmüller J 1996 *Comput. Mater. Sci.* **6** 15

[18] Kresse G and Joubert D 1999 *Phys. Rev.* B **59** 1758

[19] Blöchl P E 1994 *Phys. Rev.* B **50** 17953

[20] Bengone O, Alouani M, Blöchl P and Hugel J 2000 *Phys. Rev.* B **62** 16392

[21] Perdew J P, Chevary J A, Vosko S H, Jackson K A, Pederson M R, Singh D J and Fiolhais C 1992 *Phys. Rev.* B **46** 6671

[22] Liechtenstein A I, Anisimov V I and Zaanen J 1995 *Phys. Rev.* B **52** R5467

[23] Mills G, Jonsson H and Schenter G K 1995 *Surf. Sci.* **324** 305

[24] Ceder G, Adynolv M K and Kohn A F 1997 *Comput. Mater. Sci.* **8** 161

[25] Frayret C, Villesuzanne A, Spaldin N, Bousquet E, Chotard J N, Recham N and Tarascon J M 2010 *Phys. Chem. Chem. Phys.* **12** 15512

[26] Padhi A K, Nanjundaswamy K S and Goodenough J B 1997 *J. Electrochem. Soc.* **144** 1188

[27] Islam M S, Driscoll D J, Fisher C A J and Slater P R 2005 *Chem. Mater.* **17** 5085

[28] Hoang K and Johannes M 2011 *Chem. Mater.* **23** 3003

[29] Tripathi R, Gardiner G R, Islam M S and Nazar L F 2011 *Chem. Mater.* **23** 2278

[30] Bader R F W 1991 *Chem. Rev.* **91** 893

[31] Henkelman G, Arnaldsson A and Jónsson H 2006 *Comput. Mater. Sci.* **36** 254

[32] Sanville E, Kenny S D, Smith R and Henkelman G 2007 *J. Comp. Chem.* **28** 899

[33] Zaghib Z, Mauger A, Goodenough J B, Gendron F and Julien C M 2007 *Chem. Mater.* **19** 3740

[34] Liu Z J and Huang X J 2010 *Solid State Ionics* **57** 311

[35] Mueller T, Hautier G, Jain A and Ceder G 2011 *Chem. Mater.* **23** 3854

[36] Barpanda P, Recham N, Chotard J N, Djellab K, Walker W, Armand M and Tarascon J M 2010 *J. Mater. Chem.* **20** 1659

[37] Yamada A, Takei Y, Koizumi H, Sonoyama N and Kanno R 2006 *Chem. Mater.* **18** 804

[38] Delacourt C, Laffont L, Bouchet R, Wurm C, Leriche J, Morcrette J T M and Masquelier C 2005 *J. Electrochem. Soc.* **152** A913